LES of the flow around a circular cylinder in the critical Reynolds number region -Study on asymmetric characteristics of flow and lift -

Y. ONO[1] and T. TAMURA[2]

[1] Obayashi Corporation, Tokyo, Japan
[2] Tokyo Institute of Technology, Yokohama, Japan

ono.yoshiyuki@obayashi.co.jp

1 Introduction

The recent advancement of numerical techniques has made it possible to usually simulate the flow around bluff body. Some LES methods succeed in simulating the large scale wake structures associated with the flow separation from a circular cylinder at the sub-critical region of the Reynolds number (Re).

On the other hand, in the critical and the super critical Re regions, there appears a bubble which represents an intricate combination of laminar separation, transition, reattachment and turbulent separation of the boundary layers.

According to the previous researches, the asymmetric flow pattern coupled with steadily existing lift is recognized around a circular cylinder in the critical Re region. Bearman (1969) found that the asymmetric situation is caused by a laminar separation bubble forming on only one side of the cylinder in the critical Re region, while the symmetric situation appears as a consequence of a two-sided separation bubble in the super critical Re. Kamiya et al. (1979) also recognized the steady lift, and investigated the asymmetric pressure distributions accompanied by the shift of the stagnation point away from the bubble. Schewe (1986) measured repeatedly the sign of the steady lifts in the cases that the asymmetric flow pattern was observed, and showed that the probability for the occurrences of each sign was nearly equal. This finding showed that asymmetric phenomena were basic behavior, namely not induced by asymmetric test condition. Schewe (1983) explained the asymmetric flow was originated from local perturbations or fluctuation of the oncoming flow. The immediate formation of one side bubble results in acceleration of the fluid and in deceleration on the other side. Deceleration of the fluid delays the transitions to the turbulence and the formation of the bubble. This coupled occurrence of the development of a bubble on one side with the deceleration of the fluid on the other side causes stabilizing and fixing of the asymmetric flow situation.

Up to that time, the separation bubbles observed in the critical and the super critical Re regions were regarded as two-dimensional steady circulations. However, Schewe (1986) explains a regular three-dimensional cellular structure is observed along the cylinder in the oil-flow photographs. Furthermore, there exists the fluctuation of the lift in the critical Re region in spite that one side steady laminar separation bubble is formed. Schewe (1983) explains that the dominating vortices are those which are shed from the side where the boundary-layer transition has not yet occurred.

As reviewed by Zdravkovich (1992), many researches on the asymmetric flow pattern in the critical Re region have been reported. However, the details of the asymmetric flow characteristics such as a one side separation bubble, a laminar separated shear layer at the other side have not reached completely understanding. Especially, it is not clarified why the separation bubble is formed consistently on one same side.

The above flow characteristics are investigated by using wind tunnel experiments. It is not easy to get the flow information near the circular cylinder at high Re region. Almost all of the flow characteristics in the critical Re region are not visually captured.

On the other hand, until now, many CFD (Computational Fluid Dynamics) models have been applied to the flow around a circular cylinder near the critical Reynolds number. However, there exist few computations which can simulate the steady lift of a circular cylinder in the critical Re region. Furthermore, the complicated flow structures which induce the asymmetric flow pattern in the critical Re region have never been numerically captured.

The authors of this paper showed the LES method using very slight numerical dissipation and very fine grid resolution in the span-wise direction could capture the aerodynamic characteristics in the drag-crisis phenomena of a circular cylinder at the super critical Reynolds number (ONO& TAMURA, 2008). Also, as a result of studying the complicated flow near the separation points, the distortion of the separation bubbles was recognized at the instantaneous flow around reattachment points, while a two-dimensional separation bubble is formed in the time-averaged flow. Some

reattachment points are randomly recognized instead of two-dimensional reattachment line.

In this research, the asymmetric flow pattern coupled with steady lift around a circular cylinder in the critical Reynolds number region is investigated by using the LES method. First, adequate numerical conditions are elucidated. The influences of grid resolution on the aerodynamic quantities are examined through the comparison with the previous experiments. Next, the time-averaged asymmetric pressure and flow characteristics are investigated by using the computed results. Finally, the characteristics of one side separation bubble, a laminar separated shear layer at the other side are studied by using computed flow visualization.

Also, the unsteady wake structure associated with the fluctuation of the lift coefficient in the critical Re region is discussed.

2. PROBLEM FORMULATION

The governing equations are given by the incompressible Navier-Stokes and the continuity equations. To advance the solutions of velocities and pressure in time, a fractional step method is employed. The time integral of the momentum equation is hybrid, that is to say, the Crank-Nicolson scheme is applied to the viscous terms and the explicit third-order Runge-Kutta method is used for convective terms. Spatial derivatives of variables are treated as second-order central difference. Convective terms are approximated using the higher-order interpolation method. To avoid the numerical oscillation, very slight numerical dissipation is added to convective terms. The dynamic mixed model is used as SGS model.

3. Computational model

In order to distribute the grid points in the whole domain around a circular cylinder with a balanced size, the over-set grid system is employed. Figure 1 shows the overset grid systems near the cylinder in the present computations which are composed by three kinds of meshes. The grid points in the each mesh are shown in *Table 1*. Grid 1 was used in the previous computations (ONO, TAMURA, 2008) which succeeded in simulating the flow in the super critical Re region.

On the other hand, Grid 2 has longer grid region in the span-wise direction and Grid 3 has the much finer grid resolutions in the circumferential direction than Grid 1. Grid 2 and Grid 3 have the same grid resolution as Grid 1 in the span-wise direction.

Standard inflow conditions, $u=U$, $v=w=0$ are imposed at the upstream boundary, and the convective condition is imposed at downstream boundary. No-slip condition is used at the cylinder surface. Smallest grid size is $1.3\text{X}10^{-4}$ which is equals to $0.1/(\widetilde{\text{Re}})^{0.5}$ ($\widetilde{\text{Re}}$ = 600,000 is used in the previous paper, $\text{Re}(=UD/\nu)$ is the Reynolds number D: diameter of a circular cylinder, ν is the kinematic viscosity).

Table 1 : Computational grid points

Grid	Dir	Mesh1	Mesh2	Mesh3	lz
Grid1	x(ξ)	101	311	501	D
	y(η)	91	181	61	
	z(ζ)	31	151	151	
Grid2	x(ξ)	101	311	501	8.4D
	y(η)	91	181	61	
	z(ζ)	1261	1261	1261	
Grid3	x(ξ)	312	501	2001	2D
	y(η)	212	340	240	
	z(ζ)	301	301	301	

lz: length in the span-wise direction

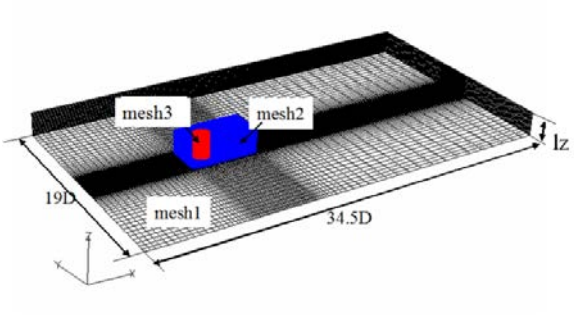

(1) Computational region

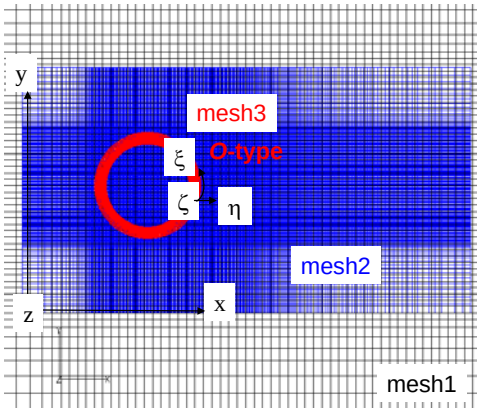

(2) Computational grid near cylinder

Figure 1: Over set grid system

4 Computaional results

4.1 Influence of numerical conditions

In 4.1, the influences of grid resolution on aerodynamic coefficients are investigated. The computed aerodynamic quantities such as time-averaged drag coefficient (C_{Dave}), lift coefficient (C_{Lave}) and the Strouhal number (St) are summarized in Table 2.

In the previous paper, the aerodynamic coefficients in the super critical ($Re=6.0X10^5$) region have been captured by using Grid 1. However, in the case at $Re=2.0X10^5$, the computations using Grids1 can't simulate appropriately the steady lift coefficient, and C_{Dave} and St in the critical Re region. The computations tend to be close to the experiments in the super critical Re region. As shown in Table 2, the computation using Grid 2 which has the grid region of 8.4 times Grid1 in the span-wise direction also can't capture the steady lift. The computations have been executed at the Re less than $2X10^5$, though the computed results are not shown in a table 2. However the steady lift has not been reproduced.

On the other hands, in the case of Grid3 using finer grid resolution in the circumferential direction, C_{Dave} at $Re=2.0x10^5$ shows agreement with experiments in the sub-critical Re region. Also, at $Re=2.2x10^5$, the present computation can capture the steady lift (C_{Lave}) and St observed in the previous experiments.

Figure 2 shows the time histories of the aerodynamic coefficients at $Re=2.2X10^5$. The time-averaged values (C_{Lave}, C_{Dave}) of C_L and C_D are around 0.95 and 0.75, respectively. The value of the computed steady lift (C_{Lave}) is beyond C_{Dave} as shown in the previous experiments, though C_{Dave} is slightly larger compared with the experiments.

Consequently, the grid resolution in the circumferential direction in addition to the span-wise direction is very important to simulate the flow around a circular cylinder in the critical Re region.

4.2 Study of averaged flow

In 4.2, the characteristics of the time-averaged pressure and flow around a circular cylinder are investigated in the critical Re region. Figure 3 shows the distribution of time-averaged pressure coefficients (C_{Pave}) on the cylinder. The contours of C_{Pave}, the contours of the stream-wise velocity and velocity vectors are shown in Figure 4.

The computed flow around a circular cylinder becomes an asymmetric situation (in upward direction in Figure 4). It is recognized the flow accelerates and levels of the negative pressure became large on the upper side. On the other hand, the flow shows a deceleration and the level of the negative pressure is small on the lower side. These characteristics of the acceleration of the flow on a one bubble side and the deceleration of the flow on the other side are discussed in Schewe (1983).

Table 2 : Computed aerodynamic coefficients

Numerical condition		Computational results		
mesh	Rex10^{-4}	$C_{D\ ave}$	C_{Lave}	St
Grids1	60	0.21	0.001	0.48
EXP(super critical)[3],[6]		0.2-0.4	0.0	0.42-0.48
Grids1	20	0.26	0.01	0.45
Grids2	20	0.22	0.0006	0.47
Grids3	20	1.2	0.01	0.21
Grids3	22	0.75	0.95	0.3
EXP(critical) [3],[6]		0.5	1.2	0.32

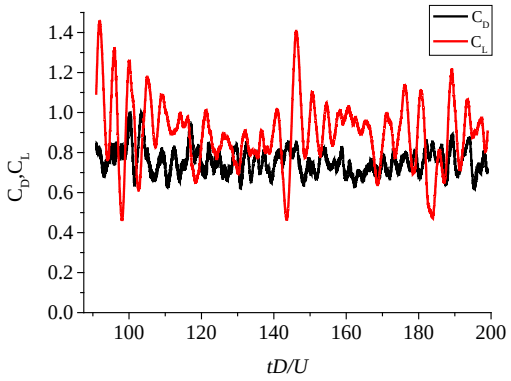

Figure 2: Time histories of aerodynamic coefficients

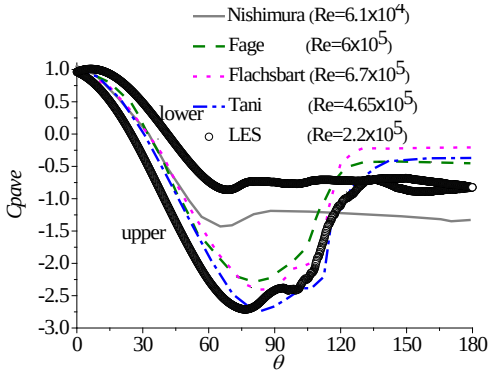

Figure 3: The distribution of time averaged pressure coefficients (C_{Pave})

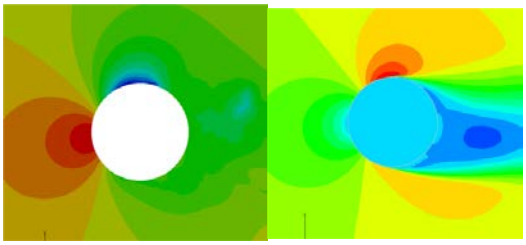

(1)Contours of C_{Pave} (2) Contours of stream-wise velocity

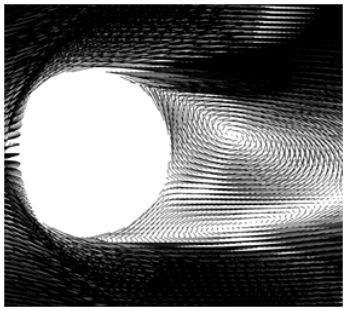

(3) Velocity vectors

Figure 4: The time-averaged flow around a circular cylinder

(The critical Re region)

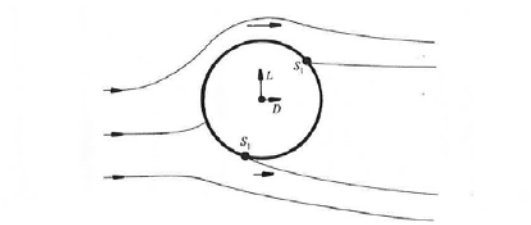

Figure 5: Simplified sketch of the asymmetric flow situation in the critical Re region

(Schewe (1983), L=lift,D=drag,St=turbulent separation,S_1=laminar separation)

The level of the negative pressure on the upper side shows more than -2.5, while it shows around -0.8 on the lower side. Concerning the base pressure, it is a middle value of those in the subcritical and the supercritical Re region, although the level of negative pressure is a little large value compared with the previous experimental result (about-0.5, Bearman, 1969).

Looking at the frontal region of the cylinder, the computed stagnation point shifts 5~10 degrees to lower side in Figure 4. This tendency is observed in the previous experimental result (Kamiya, 1979). Furthermore, as shown in Figure 3, the separation point on the upper side is located at upstream compared with that in the super critical Re region, while that on the lower side is not changed compared with that in the subcritical Re region. It is noted that the separation point on upper side is near 90 degree.

Above flow acceleration and deceleration on the both sides lead to an imbalance of the flows on between upper and lower sides. The shifts of stagnation points cause this imbalance of the volumetric flow rate to be cancelled by changing the flow on the both sides.

These characteristics of the flow in the critical Re region are in correspondence with the sketch of the asymmetric flow situation shown in Figure 5.

Schewe (1983) also investigated the wake characteristics in the critical Re region which was associated with the fluctuating lift. It was discussed that the dominating vortices in wake fluctuations were those which were shed from the side where the boundary-layer transition had not yet occurred. However, Figure 4 (3) shows the strong circulation is formed on the bubbles side (upper side), and the circulation on the other side, where the boundary-layer transition has not yet occurred, becomes weak.

4.3 Study of instantaneous flow structure in the critical Reynolds number region

(1) Flow separation and reattachment region

The separation bubbles had been regarded as two-dimensional steady circulations. However, Schewe (1986) pointed out that the two dimensional bubble was observed only in a rather coarse picture, and a regular three-dimensional cellular structure was observed along the cylinder in the oil-flow photographs.

The authors of this paper studied the flow characteristics around a circular cylinder in the super critical Re region. In the computed results, some stagnation points in the reattachment region on the both sides of the cylinder are randomly recognized in the instantaneous flow instead of two-dimensional re-reattachment line. These stagnation points become the sources of the flow, and several divergences of the flow are recognized. These divergences cause the velocities in steam-wise and span-wise direction to rapidly increase and results in distortion of the separation bubbles on the both side of the cylinder.

These flow structures might be identified with a regular three-dimensional cellular structure along the cylinder observed by Schewe (1986).

Figure 6 shows the velocity vectors near the surface of the cylinder in the critical Re region and the super critical Re region. In the critical Re region, the divergences of the flow occur on only one side. The velocities rapidly increase around the reattachment points on the bubble side.

Looking at the flow separation region, the separation line is distorted in the span-wise direction in the critical Re region, while the flow separate parallel to the axis of the span-wise direction in the super critical Re region. Furthermore, the reattachment points (boundary of the red vector and blue ones) are largely curved aslant in the critical Re region.

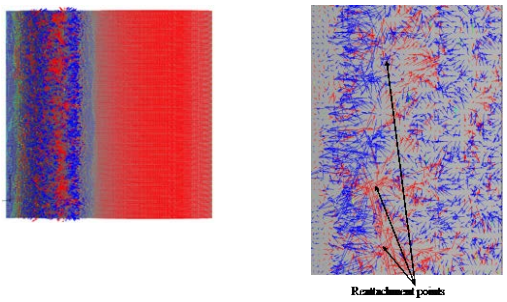

Divergence of the flow

(Enlargement)

The super critical Re region

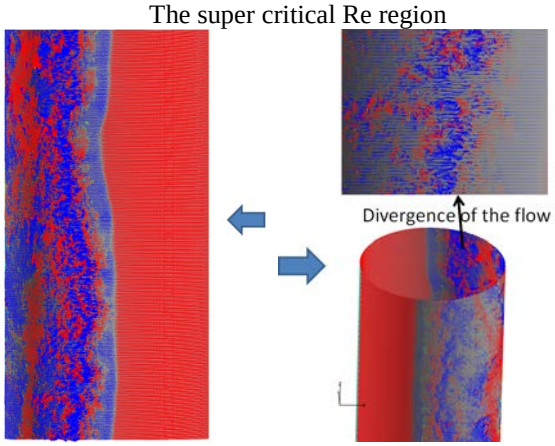

Divergence of the flow on only one side

The critaical Re region

Figure: 6 The velocity vectors near the cylinder surface

(Red vectors depicts positive velocities, the blues are negative ones)

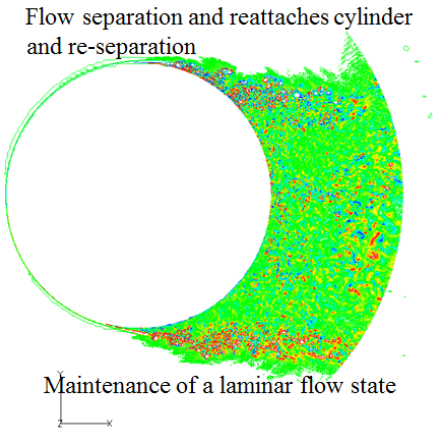

Figure 7: The contours of instantaneous vorticities around a circular cylinder in the critical Re regions.

This characteristics of the flow are probably caused by the occurrence of flow separation and reattachment near 90-degree. As explained in characteristics of time-averaged pressure distribution (Figure 3), the separation point shifts to upwind direction associated with the displacement of the stagnation point. Largely curved flow along the cylinder-surface is induced by the flow separation and reattachment near 90 degree. These flow states causes the locations of flow re-attachment points to be unstable and lead to largely curved formation of separation bubble in the span-wise direction.

Therefore, the characteristics of the one side bubble in the critical Re region have the three-dimensionality and are different quality from those of the two side bubbles in the super critical Re region.

Figure 7 shows the computed results for the contours of the vorticities around a circular cylinder at the critical Re region. On the upper side, the flow transits laminar to turbulence after flow separation, and then reattaches to the cylinder surface. On the other hand, the laminar state maintains after laminar separation on the lower side. The reattachment of the flow has never been recognized.

In mentioned in 4.1, the grid resolutions not only in the span-wise direction but also in circumferential direction are very important to simulate the flow around a circular cylinder in the critical Re region. One of the reasons which are not able to simulate an asymmetrical flow situation might be that the coarse resolution disturbs the laminar state after flow separation and leads to the flow reattachment on the both sides.

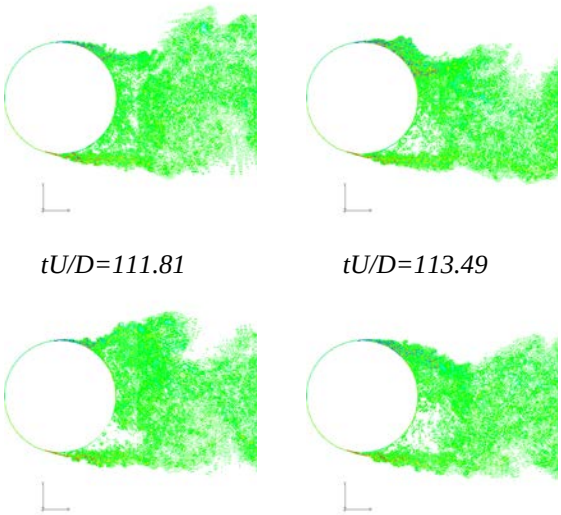

tU/D=111.81 *tU/D=113.49*

tU/D=115.13 *tU/D=116.95*

Figure 8: Time series of the contours of vortices

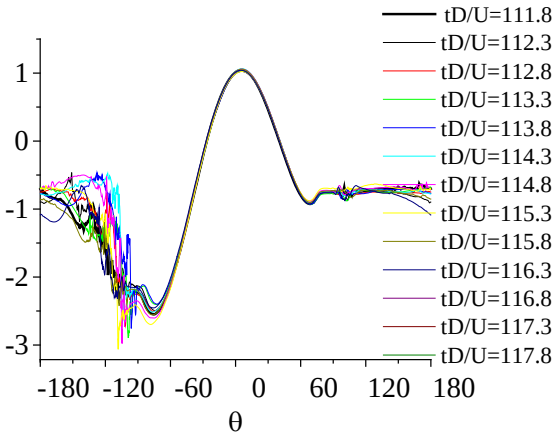

Figure 9: Time variations of the pressure distribution on the cylinder surface (Middle section)

(2) Wake region

It is well known that the asymmetrical flow pattern in the critical Re region is caused by the slight difference of the flow transition characteristics. However, it is not clarified why the slight difference of the flow leads to one side bubble consistently on the same side.

Also, the fluctuation of the lift is observed in the critical Re in spite that one side steady laminar separation bubble is formed. Therefore, the wake characteristics should be discussed in the critical Re region.

In order to investigate the unsteady characteristics of the wake vortices, the contours of vorticities around a circular cylinder are shown in Figure 8.

On the upper side, the flow reattachment and re-separation occur associated with one bubble formation. After that, the separated shear layer largely fluctuates in transverse direction, and vortices are formed near the base of the cylinder. On the other hand, the separated shear layer hardly fluctuates on lower side where the boundary-layer transition has not yet occurred. On the lower side, the inclination of the separated shear layer tends to be lost, and the vortices are formed further from the base of the cylinder.

Figure 9 shows the time variations of the pressure distribution on the cylinder surface at the middle section in the span-wise direction. There is little fluctuation on the right side where the boundary-layer transition has not yet occurred. On the other hand, on the left side, it is recognized that pressure distributions largely fluctuate in the region from reattachment points to the base of the cylinder. Namely, it is confirmed in the unsteady pressure characteristics that the dominating vortices associated with lift fluctuation are those which are shed from the side where the separation bubble is formed. To investigate the relationship between the pressure and the flow characteristics, Figure 10 shows iso-surface of instantaneous pressure and △p around a circular cylinder.

Figure 10: Iso-surface of instantaneous pressure and laplacian p

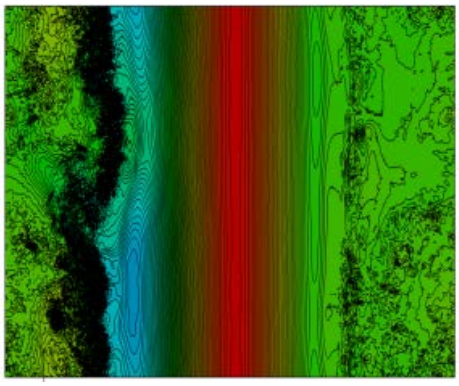

Figure 11: Contours of pressure on the cylinder surface

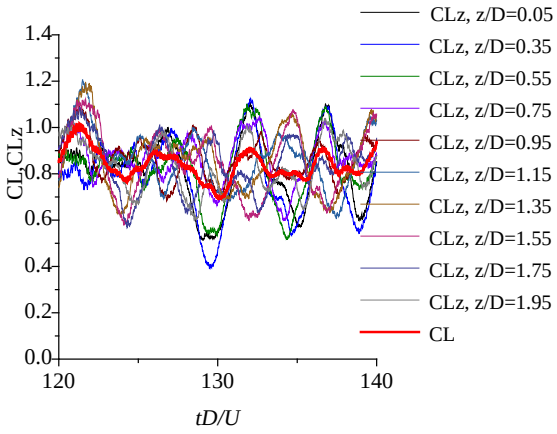

Figure 12: Time histories of the lift coefficient and the local lift coefficients (tD/U= 120~140)

Figure 11 shows the contours of pressure on the cylinder surface. A one side bubble is largely curved aslant in the whole region of span-wise direction. The inclined re-separations are recognized and bring about formation of slant vortices which are locally close to the base of the cylinder in the span-wise direction.

Figure 12 shows the time histories of the total lift coefficient and the local lift coefficients at the 10 sections (z/D=0.05~1.95) in the span-wise direction. There exists the fluctuation of the total lift coefficient. Furthermore, the local lift coefficients largely fluctuate associated with formation of the slant vortices near the base of the cylinder. On the other hand, the various fluctuations of the local lift coefficients in the

span-wise direction cause the fluctuation of total lift coefficient to decrease.

The various timings of vortex formations on the bubble side prevent the shear layer on the other side from forming toward the base of the cylinder. As a result, the separated shear layer where the boundary-layer transition has not yet occurred loses the inclination and tends to be hard to reattach to the cylinder surface. These flow characteristics on the both sides cause stabilizing and fixing of the asymmetric flow situation in the critical Re region.

5 Conclusion

The LES method is applied to the flow around a circular cylinder in the critical Re region. The LES model using fine grid resolution in the circumferential direction gives the asymmetric flow pattern and steady lift in the critical Re region. The characteristics of asymmetric flow in detail were discussed by using the computed results.

First, the dependency of the grid resolution on the steady lift coefficients was examined through comparison of the computed results of three type of the mesh. In the case of using the fine grid resolution in the circumferential direction in addition to the span-wise direction, the asymmetric flow situation in the critical Re region could be captured. The large value of the steady lift beyond to the drag coefficients was simulated.

Time-averaged flow and pressure distributions were investigated in the critical Re region. The asymmetric distribution of the time-averaged pressure coefficients and time-averaged asymmetric flow situation are simulated by the present simulation. It is confirmed that the flow accelerates and levels of the negative pressure became large on the bubble side, while the flow shows a deceleration and the level of the negative pressure is small on the other side. The computed stagnation point shifts 5~10 degrees to the other side as observed in the previous experimental results. Above flow acceleration and deceleration on the both sides lead to an imbalance of the flows on between upper and lower sides. The shifts of stagnation points cause this imbalance of the volumetric flow rate to be cancelled by changing the flow on the both sides. These characteristics of the flow in the critical Re region are in correspondence with the sketch of the asymmetric flow situation shown in the previous research (Schewe, 1983).

On the other hand, in the previous research, concerning the lift fluctuation in the critical Re region, the dominant vortices in wake fluctuations are those which are shed from the side where the boundary-layer transition has not yet occurred. However, the strong circulation is formed on the bubbles side, and the circulation on the other side, where the boundary-layer transition has not yet occurred, becomes weak. The dominant vortices associated with lift fluctuation are those which are shed from the side where the separation bubble is formed.

The asymmetric flow situation in the critical Re region is brought about by the interaction of the both side of the flow around a circular cylinder. The flow separation and reattachment occur near 90-degree associated with the shift of a stagnation point to the laminar side. Largely curved flow along the cylinder-surface causes the locations of flow re-attachment points in the span-wise direction to be unstable. The various location of the reattachment points lead to largely curved formation of separation bubble. These characteristics near the flow separation and reattachment region results in the formations of the aslant scattered vortices in the wake of the cylinder. The various timings of the vortex formation in the span-wise direction on the bubble side prevent the shear layer on the other side from forming near the base of the cylinder. The separated shear layer where the boundary-layer transition has not yet occurred loses the inclination and tends to be hard to reattach. These flow characteristics on the both sides cause stabilizing and fixing of the asymmetric flow situation in the critical Re region.

Acknowledgements

The computations in this paper were performed by using Earth Simulator 2 in JAMSTEC.

References

G., Schewe, On the force fluctuations acting on a circular cylinder in cross flow from subcritical up to trans critical Reynolds number, Journal Fluid mech., 133, 1983, pp265-286

G., Schewe, “Sensitivity of transition phenomena to small perturbations in flow round a circular cylinder”, J. Fluid Mech., 172, 33(1986)

K., Kamiya, S., Suzuki, R., Nishi, “ On the aerodynamic force acting on circular cylinder in the critical range of the Reynolds number,” ALAA paper 79-1475.Williamsburg, (1979).

M.M. Zdravkovich, Flow around Circular Cylinders, Vol1, Oxford university press, 19

P.W., Bearman, On vortex shedding from a circular cylinder in the critical Reynolds number region. Journal Fluid Mechanics, 37, pp577-587, 1969.

T., Tamura, K., Kuwahara and I., Ohta, “On reliability of the two-dimensional computation for the cylindrical-type structure”, J. Wind Eng. Ind. Aerodyn.,35 (1990).

Y., Ono, T., Tamura,“ Large eddy simulation using a curvilinear coordinate system for the flow around a square cylinder,” Wind&Structure,Vol5, No2, 369-378 (2002).

Y.,Ono,T.,Tamura, LES of flows around a circular cylinder in the critical Reynolds number region, Proc. of BBAA VI International CollOQUIUM, MILANO, ITALY, JULY, 20-24 2008 (http://bbaa6.mecc.polimi.it/uploads/validati/ccn06).